This is an author-deposited version published in: http://oatao.univ-toulouse.fr/
Eprints ID: 3222

To cite this document: SIMOES Alberto, ALAZARD Daniel, TUAN Hoang, APKARIAN Pierre. Lateral fligh control design for a highly flexible aircraft using a nonsmooth method. In: *48th IEEE Conference on decision and control*, 16-18 Dec 2009, Shanghai, China.

Any correspondence concerning this service should be sent to the repository administrator: staff-oatao@inp-toulouse.fr

Lateral fligh control design for a highly flexibl aircraft using a nonsmooth method

A. M. Simões, D. Alazard, H. D. Tuan and P. Apkarian

Abstract— **This paper describes a nonsmooth optimization technique for designing a lateral fligh control law for a highly flexibl aircraft. Flexible modes and high-dimensional models pose a major challenge to modern control design tools. We show that the nonsmooth approach offers potent and flexibl alternatives in this difficul context. More specificall , the proposed technique is used to achieve a mix of frequency domain as well as time domain requirements. For a set of different fligh conditions.**

I. INTRODUCTION

The synthesis of fligh control laws for modern aeronautics and space applications remains a challenging task whenever aeroservoelastic phenomena significantl affect the control bandwidth. Such phenomena are especially critical when demanding specification including performance and robustness constraints of different natures must be achieved. Performance specifications for instance, are normally related to control objectives like tracking and decoupling and are naturally expressed in terms of time-domain constraints such as limited overshoot, short settling- or rise-times, small steady-state error and amplitude limitation. Flexible modes, on the other hand, are frequently dealt with via frequency-domain criteria or modal specification (prescribed damping ratios). A further complication is related to structural constraints imposed to the controller. Simpler controllers are generally sought to facilitate on-board implementation and management.

The classical approach in which a control law is designed for the rigid dynamics and a low-pass filte is inserted a posteriori to avoid or reduce spillover effects is no longer a valid scheme for such applications. The reason is that in order to meet appropriate level of performance, the controller bandwidth should overlap with the frequency range of fl x-ible modes which represents a core issue of such problems.

Traditional H_2 or H_∞ syntheses as described in the standard textbook [19] do not provide suitable answers to these difficulties First of all, time-domain specification should be addressed indirectly via nontrivial tuning of weighting filters Secondly, these methods produce full-order controllers and

A. M. Simões is with Control System Department, ONERA-CERT, 2 av. Edouard Belin - 31055 Toulouse, France alberto.simoes@cert.fr

D. Alazard is with ISAE, 10 av. Edouard Belin - 31055 Toulouse Cedex, France, alazard@isae.fr

H. D. Tuan is with School of Electrical Engineering & Telecommunications, UNSW, Sydney, Australia, h.d.tuan@unsw.edu.au

P. Apkarian is with Control System Department, ONERA-CERT, 2 av. Edouard Belin, 31055 and Université Paul Sabatier, Institut de Mathématiques, Toulouse, France, apkarian@cert.fr

therefore rely on model reduction techniques to derive simple controllers which is always prone to failure.

Design methods based on the Youla parametrization [8] offer some fl xibility to handle both time- and frequency-domain specifications The resulting controllers however suffer from substantial size inflatio and are hardly amenable to numerical implementation.

Different approaches have been reported in the literature trying to exploit eigenstructure assignment methods to design problems involving lightly-damped fl xible modes [11], [12], [15]. Eigenstructure assignment methods are interesting because they allow to capture time-domain specification through modal shaping. Unfortunately, as noted in [11], determining appropriate eigenspaces associated with fl xible modes remains an inherent difficult .

Nonsmooth optimization techniques have been used recently to solve a number of difficul structured controller design problems involving time- or frequency-domain specifications see [2], [3], [7], [10], [16] and references therein. The nonsmooth design method considered here bear the following appealing features. First, time-domain specifica tions are addressed directly, thus dispensing with the use of auxiliary tuning parameters such as weighting filters More-over, frequency-domain constraints such as those related to fl xible modes are easily incorporated within the same framework. Secondly, such techniques remain operational even for large size plants, and thus allow to short-circuit risky model reduction phases. Finally, they encompass arbitrary controller structures which make them methods of choice when implementation constraints are important.

The central aim of the present work is to illustrate the efficien y and the fl xibility of nonsmooth design methods in solving difficul structured control design problems like large size fl xible transport aircraft.

The paper is organized as follows. Section II discusses the multi-objective control design problem and outlines key ingredients of the proposed nonsmooth optimization technique. The difficul design problem of lateral fligh control for a highly fl xible aircraft subject to turbulence and multiple load conditions is addressed in Section III.

NOTATION

We use $\mathbb{R}^{n \times m}$ to denote the space of $n \times m$ real matrices. The symbol $\alpha(M)$ stands for the spectral abscissa of a matrix $M \in \mathbb{R}^{n \times n}$ and is define as $\alpha(M) := \max \{\text{Re } \lambda : \lambda \text{ eigenvalue of M }\}$. The $\max$ operator applied to a vector $v \in \mathbb{R}^n$ is define as $\max v = \max\limits_{i=1,\ldots,n} v_i$. The notation $[.]_+$ applied to a scalar α denotes the threshold

function $[\alpha]_+ = \max\{0, \alpha\}$. Its generalization to a vector $v \in \mathbb{R}^n$ is define as $[v]_+ = \max\{0, \max v\} = \max\limits_{i=1,\ldots,n} [v_i]_+$. Important concepts from nonsmooth analysis are covered by Clarke in [9]. For a locally Lipschitz function $f : \mathbb{R}^n \to \mathbb{R}$, $\partial f(x)$ denotes its Clarke subdifferential at x while $f'(x;h)$ stand for its directional derivative at x in the direction h. For functions of two variables $f(x,y)$, $\partial_1 f(x,y)$ will denote the Clarke subdifferential with respect to the firs variable. For differentiable functions f of two variables x and y the notation $\nabla_x f(x,y)$ stands for the gradient with respect to the firs variable. The symbol $\mathcal{F}_l(.,.)$ will refer to the classical lower Linear Fractional Transformation [19, Ch. 10].

II. MULTI-OBJECTIVE CONTROLLER DESIGN VIA NONSMOOTH OPTIMIZATION
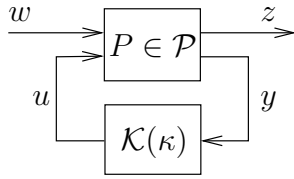

Fig. 1. Synthesis closed-loop interconnection

To begin with, consider the synthesis interconnection given by the standard form in Figure 1 with $u \in \mathbb{R}^{m_2}$ and $y \in \mathbb{R}^{p_2}$ and where the multivalued plant $P(s)$ takes values in a finit family of linear plants $\mathcal{P} := \{P^1, \ldots, P^p\}$ representing, for instance, multiple operating conditions or faulty modes. Each plant $P \in \mathcal{P}$ is described by a minimal state-space realization of the form

$$\begin{bmatrix} \dot{x}(t) \\ z(t) \\ y(t) \end{bmatrix} = \begin{bmatrix} A & B_1 & B_2 \\ C_1 & D_{11} & D_{12} \\ C_2 & D_{21} & D_{22} \end{bmatrix} \begin{bmatrix} x(t) \\ w(t) \\ u(t) \end{bmatrix}, \qquad (1)$$

where indexing has been removed for simplicity. In order to address practical controller structures we introduce a state-space parametrization of the form

$$\kappa \in \mathbb{R}^q \to \mathcal{K}(\kappa) := \begin{bmatrix} A_K(\kappa) & B_K(\kappa) \\ C_K(\kappa) & D_K(\kappa) \end{bmatrix} \qquad (2)$$

with corresponding frequency-domain representation

$$K(s, \kappa) = C_K(\kappa)(sI - A_K(\kappa))^{-1} B_K(\kappa) + D_K(\kappa),$$

where $A_K \in \mathbb{R}^{k \times k}$. In the above description, κ designates the decision vector of design variables in the controller. Note the case of a static controller ($k = 0$) is a particular instance. The mapping $\mathcal{K} : \mathbb{R}^q \to \mathbb{R}^{(m_2+k) \times (p_2+k)}$ is assumed to be continuously differentiable but otherwise arbitrary.

Performance specification are given in most cases in terms of time-domain constraints like limited overshoot, short settling- or rise-times, but also amplitude limitation in order to guarantee decoupling properties or to avoid reaching operational limits of the system. Specification on such time-domain characteristics are achieved by direct shaping of closed-loop system responses to fi ed test input signals.

More specificall , we assume each plant in the family $\mathcal{P}$ in feedback loop with the controller $K(s)$ is subject to one or several input signals w selected in a finit signal generator set $\mathcal{W} := \{w^1, \ldots, w^d\}$. This gives rise to a finit family of closed-loop responses $z \in \mathcal{Z}$, where $\mathcal{Z} := \{z^1, \ldots, z^r\}$. Each instance in $\mathcal{Z}$ is called a scenario. Practically speaking, the signal generator set is made of typical deterministic test inputs such as steps, ramps, sinusoids, etc.

The above description is fl xible enough to reflec situations in which a single plant is submitted to various test signals as in the case when decoupling properties must be examined, or when the response to a given test signal is to be considered for multiple operating conditions or faulty modes. The proposed set-up also accepts more complicate formulations where each plant in the family $\mathcal{P}$ is tested against several inputs.
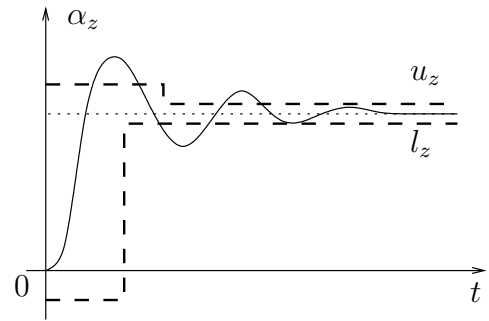

Fig. 2. envelop constraints on the step response

The goal is to compute $\kappa \in \mathbb{R}^q$ such that the closed-loop time responses $z \in \mathcal{Z}$ obtained with controller $\mathcal{K}(\kappa)$ meet envelope constraints of the form

$$l_z(t) \leq z(t) \leq u_z(t), \ \forall t \geq 0, \ \forall z \in \mathcal{Z}, \qquad (3)$$

where l_z and u_z are lower and upper bounds for z and are assumed piecewise constant in the sequel. These bounds are illustrated as dashed lines in Figure 2 for a step following specification

On the other hand, design specification like robustness against exogenous bounded-energy disturbances or unstructured uncertainties are known to be better addressed by frequency-domain criteria like bounds on the maximum singular value norm of suitable closed-loop transfers. Therefore, in addition to the constraints in (3), the designed controller $\mathcal{K}(\kappa)$ is required to achieve prescribed bounds for a finit set of closed-loop transfers

$$\|\mathcal{F}_l(P(s), K(s, \kappa))\|_{I_P} \leq \gamma_P, \ \gamma_P > 0, \ \forall P \in \mathcal{P}^\infty, \ \mathcal{P}^\infty \subset \mathcal{P}, \qquad (4)$$

where $\|.\|_{I_P}$ denotes the peak value of the transfer function maximum singular value norm on a prescribed frequency interval I_P:

$$\|\mathcal{F}_l(P(s), K(s, \kappa))\|_{I_P} := \sup_{\omega \in I_P} \overline{\sigma}(\mathcal{F}_l(P(j\omega), K(j\omega, \kappa))).$$

The frequency band I_P is typically a closed interval $I_P = [\omega_1^P, \omega_2^P]$, or more generally, a finit union of intervals $I_P =$

$[\omega_1^P,\,\omega_2^P]\cup\ldots\cup[\omega_q^P,\,\omega_{q+1}^P]$, where right interval tips may take infinit values. Alternatively, a static dynamic weight can be included in (4) if necessary

$$\|W_P(s)\mathcal{F}_l\left(P(s),K(s,\kappa)\right)\|_{I_P}\leq 1,\;\forall P\in\mathcal{P}^\infty,\;\mathcal{P}^\infty\subset\mathcal{P}. \tag{5}$$

to stress the relative importance of each channel.

Finally, the most fundamental specificatio for a closed-loop system is internal stability. Thus, the sought controller $\mathcal{K}(\kappa)$ must also guarantee negative upper bounds on the closed-loop spectral abscissas

$$\alpha(\mathcal{A}_P(\kappa))\leq\alpha_P,\;\alpha_P<0,\;\forall P\in\mathcal{P}, \tag{6}$$

where $\mathcal{A}_P(\kappa)$ is the state matrix of the closed-loop system $\mathcal{F}_l\left(P(s),K(s,\kappa)\right)$.

In summary, the considered multi-objective controller design problem may be stated as: fin controller variables $\kappa\in\mathbb{R}^q$ such that constraints (3)-(6) are satisfied In what follows it is discussed how to solve this problem. Notice, initially, that the time-domain constraints in (3) are automatically met if function

$$f_t(\kappa):=\max_{z\in\mathcal{Z}}\max_{t\geq 0}\left\{[z(\kappa,t)-u_z(t)]_+,\;[l_z(t)-z(\kappa,t)]_+\right\} \tag{7}$$

is non-positive. Similarly, the frequency-domain constraints in (4) and the spectral constraints in (6) are satisfie if functions

$$f_\infty(\kappa):=\max_{P\in\mathcal{P}^\infty}\frac{\|\mathcal{F}_l\left(P(s),K(s,\kappa)\right)\|_{I_P}}{\gamma_P}-1 \tag{8}$$

and

$$g_\alpha(\kappa):=\max_{P\in\mathcal{P}}\left(\alpha(\mathcal{A}_P(\kappa))-\alpha_P\right), \tag{9}$$

are also non-positive, respectively.

The nonsmooth design method is thus based on solving the max-type optimization problem

$$\begin{aligned}&\underset{\kappa\in\mathbb{R}^q}{\text{minimize}}&&f(\kappa):=\max\left\{f_t(\kappa),f_\infty(\kappa)\right\}\\&\text{subject to}&&g_\alpha(\kappa)\leq 0,\end{aligned} \tag{10}$$

Note a feasible solution κ^* to (10) also solves the original multi-objective design problem whenever the fina objective value $f(\kappa^*)$ is non-positive. In case $f(\kappa^*)$ is positive, a restart with a different seed will be required if the specification set (3)-(6) are to be kept unchanged because the proposed technique only provides local solutions.

Notice that program (10) is nonconvex, nonsmooth and semi-infinite and therefore represents a difficul mathematical programming problem. Instead of using alternative smooth formulations which can be very expansive computationally, see [13] for an example, a specialized nonsmooth optimization technique presenting global convergence properties and allowing to solve (10) directly has been developed in [3]. Global convergence refers here to the convergence towards a locally optimal solution from an arbitrary, even remote, starting point.

Program (10) can be seen as a Chebyshev norm-based scalarization of the original multi-objective design problem in which the role of individual weights for the various specifi cations is played by the tuning parameters l_z, u_z, γ_P and α_P. The strategy adopted here to select these weights is close in spirit to the aspiration levels approach for multi-objective optimization [8, p.64]. The tuning parameters are then adjusted iteratively based on a few trial-and-error designs: satisfie constraints can be strengthened while violated constraints can be relaxed. Indeed, one of the appealing features of the present design method is that tuning parameters are closely related to engineering specifications so that their adjustment is fairly straightforward.

The design framework given by program (10) and the non-smooth optimization technique discussed bellow is fl xible enough to accommodate an even richer set of specifications We refer the reader to [4] for further examples. At this stage it is important to emphasize that program (10) does not involve any Lyapunov variables as would be the case if LMI formulations were used. The size of such variables grows quadratically with the plant dimension which is a major impediment for application to realistic problems. As we shall see later the proposed nonsmooth method continues to perform well for high-order plants.

A. Nonsmooth optimization technique

Initially, a strictly feasible point for program (10) is found using the results in [6]. For α_P close to zero in (9), this is essentially equivalent to findin a controller $K(s,\kappa)$ that simultaneously stabilizes in closed-loop all the models in $\mathcal{P}$.

Next, program (10) is solved based on a simplifie form of the progress function introduced by Polak [14]:

$$F(\kappa^+,\kappa)=\max\{f(\kappa^+)-f(\kappa);g_\alpha(\kappa^+)\}, \tag{11}$$

where κ represents the current iterate and κ^+ the next iterate or a candidate to become the next iterate. The key fact about the progress function (11) is that critical points $\bar{\kappa}$ of $F(\cdot,\bar{\kappa})$ will also be critical points of the original program (10) [3], [14].

The following iterative procedure is used in order to determine a point $\bar{\kappa}$ giving $0\in\partial_1 F(\bar{\kappa},\bar{\kappa})$. Suppose the current iterate κ is such that $0\notin\partial_1 F(\kappa,\kappa)$, which implies that it is possible to reduce the function $F(\cdot,\kappa)$ in a neighborhood of κ, that is, to fin κ^+ such that $F(\kappa^+,\kappa)<F(\kappa,\kappa)$. Replacing κ by κ^+, the procedure is repeated. Unless $0\in\partial_1 F(\kappa^+,\kappa^+)$, in which case a critical point has been attained, it is possible again to fin κ^{++} such that $F(\kappa^{++},\kappa^+)<F(\kappa^+,\kappa^+)$, etc. The sequence $\kappa,\kappa^+,\kappa^{++},\ldots$ so generated is expected to converge to the sought local minimum $\bar{\kappa}$ of (10).

The initial κ being strictly feasible, all consecutive iterates will remain inside the feasibility region and, consequently, inside the stability region. To realize that, notice that $F(\kappa,\kappa)=0$, so the left hand branch in (11) is active at κ. Since the new κ^+ is such that $F(\kappa^+,\kappa)<F(\kappa,\kappa)=0$, one necessarily has $g(\kappa^+)\leq F(\kappa^+,\kappa)<0$, which means that κ^+ is also strictly feasible. Moreover, this also means that the objective is minimized, since $f(\kappa^+)-f(\kappa)\leq F(\kappa^+,\kappa)<0$. By forcing iterates to remain in the stability region, one

guarantees that the algorithm will progress in a region where function f_∞ in (8) is well defined

Finding the descent step κ^+ away from the current κ is based on solving the tangent program at κ

$$\underset{d\kappa\in\mathbb{R}^q}{\text{minimize}}\ \widehat{F}(\kappa + d\kappa, \kappa) + \frac{\delta}{2}\|d\kappa\|^2, \quad \delta > 0, \qquad (12)$$

whose name is derived from the fact that a first-orde approximation $\widehat{F}(\cdot, \kappa)$ of $F(\cdot, \kappa)$ is built. Solving the tangent program provides a descent direction $d\kappa$ at κ, that is, $d_1 F(\kappa, \kappa; d\kappa) < 0$, where $d_1 F$ denotes the directional derivative of $F(\cdot, \kappa)$ at κ in direction $d\kappa$. The next iterate is then $\kappa^+ = \kappa + d\kappa$, or possibly $\kappa^+ = \kappa + \alpha d\kappa$ for a suitable stepsize $\alpha \in (0, 1)$ found by a backtracking line search. The quadratic term in (12) can be used to capture second-order information, or it may be interpreted as a trust region radius management parameter. Program (12) can be equivalently formulated as a standard convex quadratic program (CQP), which can be efficientl solved using currently available state-of-the-art codes.

In order to build the first-orde approximation $\widehat{F}(\cdot, \kappa)$ of $F(\cdot, \kappa)$ used in (12), one need initially to gather first-orde information on the various specification represented by f_t, f_∞ and g_α. For the spectral abscissa specificatio in g_α, the subdifferential of the function $\partial(\alpha \circ \mathcal{A}_P)(\kappa)$ has been given in [6]. Subgradients computation involves only basic linear algebra operations and therefore can be performed very efficientl . The subdifferential of the maximum singular value norm appearing in f_∞ shares a similar structure [2], [16]. Finally, subgradients computation for f_t relies on closed-loop simulations which can be performed very efficientl for LTI systems, the reader is referred to [7] for details.

III. Application to Lateral Flight Control Design of a Highly Flexible Aircraft

The nonsmooth method is used in this section to design a fligh controller for the lateral motion of a large carrier aircraft in which fl xibility has been intentionally degraded to a highly critical level in order to build a difficul control problem and to test the efficien y of various modern techniques. It is a difficul and realistic problem which has been initially presented in [1]. Six linearized models of the lateral motion of the aircraft around equilibrium points are considered here, corresponding to six distributions of the mass inside the plane under the same fligh condition.

Each model is described by a 68th-order state-space representation whose state vector contains 4 rigid states (yaw angle β, roll rate p, yaw rate r and roll angle ϕ), 36 states corresponding to 18 fl xible modes, 20 secondary states representing the dynamics of servocontrol surfaces and aerodynamic lags, and 8 states modeling turbulence as exogenous disturbance. There are two control inputs, given by aileron deflectio δ_l and rudder deflectio δ_n, and one exogenous disturbance input v representing gusts. For the sake of comparison, the same six measurements used in [1] are also used here, which are the roll rate p_6 and angle ϕ_6 measured at the center of the plane, the yaw rates r_1 and r_{11} at the front and the rear of the aircraft, respectively, and the

lateral accelerations n_{y7} and n_{y9} measured at two different points of the fuselage. This set of measurements was selected according to observability properties of the rigid model and firs fl xible modes (in an increasing order of pulsation) with respect to sensors location along the fuselage.

The following design specification are define for this problem:

S1 flyin quality requirements represented by time-domain templates on the step responses with respect to β and ϕ,

S2 large Dutch roll damping ratio,

S3 no degradation, or preferably improvement in damping ratios of fl xible modes,

S4 improved comfort during turbulence. The comfort performance index is measured on the frequency response of transfers between the gust v and lateral accelerations at the front, the middle and the rear of the fuselage,

S5 robustness with respect to the various loading conditions,

S6 to facilitate on-board implementation a reduced-order controller order is desirable.

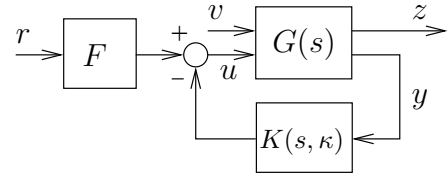

Fig. 3. closed-loop interconnection for fl xible aircraft

The adopted control configuratio and the corresponding synthesis interconnection are depicted in Figure 3, where $G(s)$ represents the aircraft transfer matrix for a given load condition, $u = \begin{bmatrix} \delta_l & \delta_n \end{bmatrix}^T$ are the control inputs, $y = \begin{bmatrix} n_{y7} & n_{y9} & p_6 & r_1 & r_{11} & \phi_6 \end{bmatrix}^T$ are the measured outputs and $r := \begin{bmatrix} \beta_r & \phi_r \end{bmatrix}^T$ is the reference vector. Different outputs will be selected so as to form the regulated output vector z according to the various criteria.

Using the fl xibility provided by parametrization (2), the feedback controller $K(s, \kappa)$ is selected a 10th-order state-space system, which means that the reduced controller order specificatio (S6) is ensured. For comparison, it should be noticed that the controller order obtained in [1] using model reduction techniques was 20. Additionally, the feedback controller is forced to be strictly proper ($D_K(\kappa) \equiv 0$ in (2)) in order to improve robustness with respect to high frequency fl xible modes and achieve better noise attenuation. The feedforward controller $F \in \mathbb{R}^{2\times2}$ is selected as a static matrix gain again for simplicity.

The firs time-domain specificatio in (S1) which is imposed on the fina closed-loop system is the steady-state constraint

$$\lim_{t\to\infty} \begin{bmatrix} \beta(t) \\ \phi(t) \end{bmatrix} = \begin{bmatrix} 1 & 0 \\ -1 & 1 \end{bmatrix} \lim_{t\to\infty} \begin{bmatrix} \beta_r(t) \\ \phi_r(t) \end{bmatrix}. \qquad (13)$$

This constraint can be addressed via appropriate selection of the pre-filte gain F. Indeed, notice that (13) will be

automatically met if F is derived through

$$F = \mathcal{F}_l \left(G_{\beta\phi}(0), -K(0,\kappa) \right)^{-1} \begin{bmatrix} 1 & 0 \\ -1 & 1 \end{bmatrix}, \qquad (14)$$

where $G_{\beta\phi}(s)$ is the open-loop transfer matrix from $\begin{bmatrix} u^T & u^T \end{bmatrix}^T$ to $\begin{bmatrix} [\beta & \phi] & y^T \end{bmatrix}^T$ and assuming existence of the inverse matrix. In practice, (14) can be written equivalently as

$$F = \mathcal{F}_l \left(M, K(0,\kappa) \right) \begin{bmatrix} 1 & 0 \\ -1 & 1 \end{bmatrix}, \qquad (15)$$

where matrix M is such that

$$\mathcal{F}_l \left(M, K(0,\kappa) \right) = \mathcal{F}_l \left(G_{\beta\phi}(0), -K(0,\kappa) \right)^{-1},$$

Existence of matrix M is guaranteed by the fact that the open-loop transfer matrix from u to $\begin{bmatrix} \beta & \phi \end{bmatrix}$ is non-singular [19, p.242]. The feedforward gain F is thus uniquely determined by the design variables vector κ via the continuously differentiable parametrization (15), which can be easily incorporated into the nonsmooth method framework. Consequently, both feedback and feedfoward controllers will be designed simultaneously throughout the optimization.

As discussed in Section II, the time-domain templates translating flyin quality requirements in (S1) are handled directly within the nonsmooth method. Two basic scenarios are initially considered. In the firs scenario, a unit step is applied to reference β_r while v and ϕ_r are considered to be zero, and appropriate envelope constraints are imposed on the relevant outputs. Figure 4 depicts the envelope constraints imposed on rigid β and ϕ for this scenario, as well as the evolution of the system responses throughout the optimization sequence, starting from the initial stabilizing controller. Notice that constraints such as minimal phase response for ϕ can be addressed easily via time-domain templates. The second scenario consists in a unitary step being applied to ϕ_r while the other two inputs are kept to zero. The corresponding envelope constraints imposed on rigid β and ϕ are depicted in Figure 5.

In order to improve performance robustness with respect to load variation, as required by (S5), the above scenarios are considered for two extreme load conditions: the lightest and the heaviest models. In the framework of Section II, this means that the plant family $\mathcal{P}$ will consist of two models which we refer to by light and heavy. Correspondingly, two different test inputs as discussed previously will be applied to both plants. This result in a total of four scenarios which must ne adequately controlled. The main idea here is that by guaranteeing similar system responses even under extreme load variations, satisfactory closed-loop system behavior can also be expected for intermediate conditions. If, however, fina closed-loop system response proves to be unsatisfactory for a given intermediate load condition, one may alternatively restart the design but this time taking the critical intermediate scenario into account via an enriched plant family $\mathcal{P}$. Analogously, constraints are imposed via (9) on the closed-loop spectral abscissas with both light and heavy models to achieve stability robustness requirements.
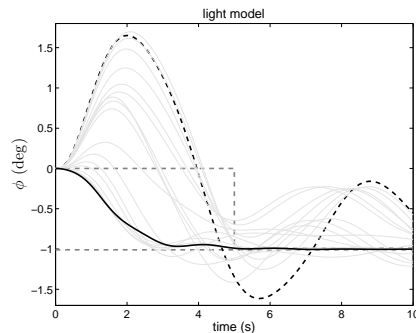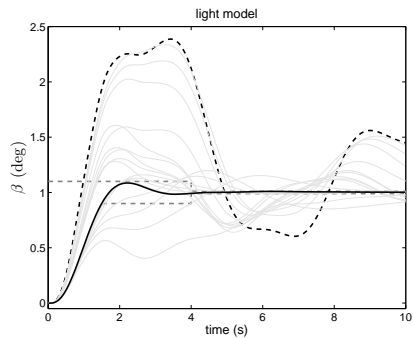

Fig. 4. Progress of closed-loop responses to a step on β_r (dashed: initial stabilizing controller, solid: fina controller)

The feedforward gain F is not depending on load conditions, so a nominal model has to be define in (14): the light model has been selected to play this role. Notice, however, that the case of an adaptive gain could also be easily handled: the only change necessary would be to consider in (14) the transfers $G_{\beta\phi}$ accordingly.

Improvement in comfort during turbulence is obtained by minimizing, in the fl xible modes frequency range, the magnitude of the transfer functions from the exogenous disturbance v to the lateral acceleration measured at three distinct points of the fuselage: front (n_{y1}), center (n_{y6}) and rear (n_{y11}). Figure 6 shows the corresponding transfer magnitudes for the uncontrolled plant and the corresponding achieved closed-loop frequency responses. Horizontal dashed lines in Figure 6 materialize bounds which have been prescribed via γ_P in (8). These frequency-domain constraints are the same for both light and heavy models in order to improve robustness with respect to load variations.

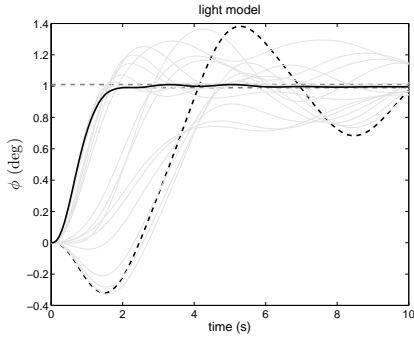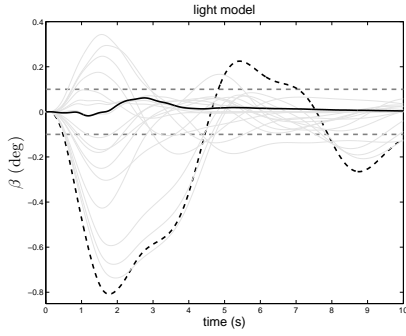Finally, norm constraints (5) are imposed on the sensitivity

Fig. 5. Progress of closed-loop responses to a step on ϕ_r (dashed: initial stabilizing controller, solid: fina controller)

function $S = (I + G_y K)^{-1}$, $G_y(s)$ being the open-loop transfer from u to y, for both light and heavy models. In addition to increasing the stability margin, these constraints allows to increase the damping ratios of the Dutch roll and the fl xible modes. The largest singular-value of S is depicted in Figure 7 for both light and heavy loads. The dotted-lines in Figure 7 represent the corresponding desired norm-bounds define via dynamic weights W_P in (5).

It is well-known that pole-zero cancellations is a critical issue when designing controllers with frequency domain techniques. Incorporating various load conditions in the synthesis is a simple device to overcome cancellations of fl xible modes. In the same vein, the possibility to work with low-order controllers (order 10 as compared to the plant order of 68) is another favorable feature to prevent pole/zero cancellations. The H_2/PRLQG criterion used in [1] to increase the damping ratios of fl xible modes is another potential option which requires constructing a linear fractional representation to model parametric uncertainty in
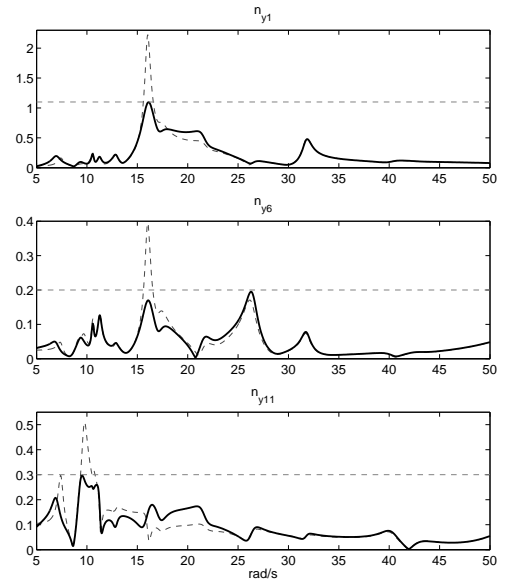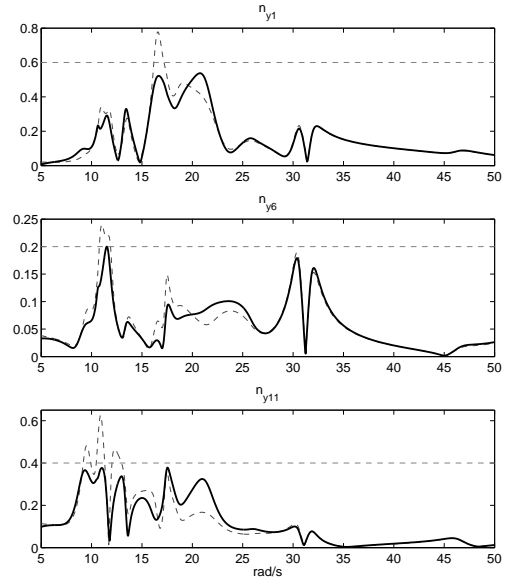
(a) light   (b) heavy

Fig. 6. Magnitudes of the transfers from v to lateral accelerations (dashed: open-loop plant, solid: fina closed-loop)

fl xible modes. We have not followed this route here as LFR models suggest using μ-synthesis as design tool with the difficultie discussed above in terms of controller order and structure.

Figure 8 depicts the position of closed-loop poles in the complex plane as the controller gain is varied from 0 to 100%. As required, the Dutch roll damping ratio has been significantl increased, as well as the damping ratios of the firs fl xible modes. Additionally, no critical damping ratio
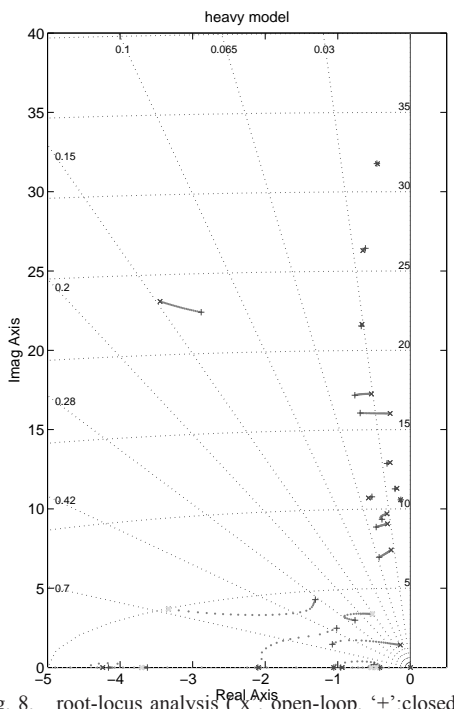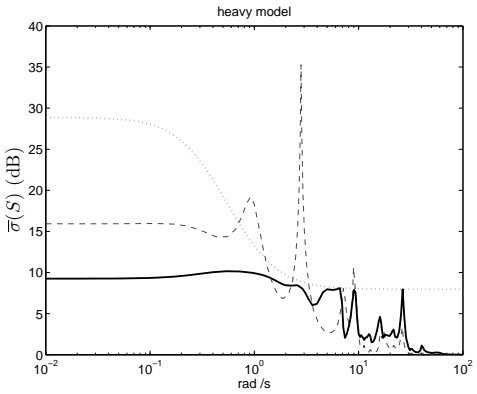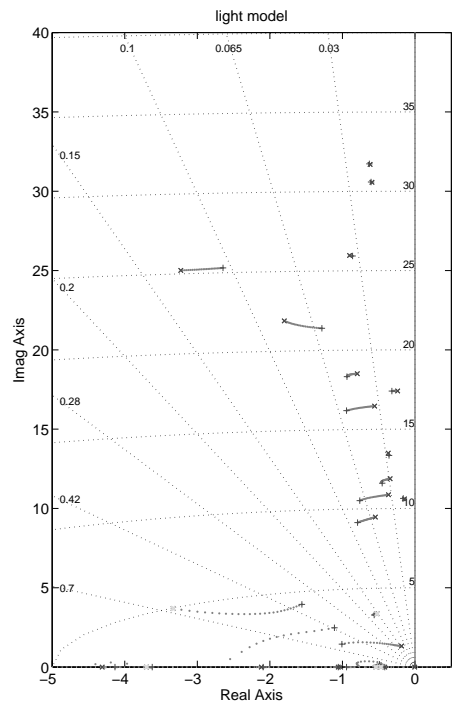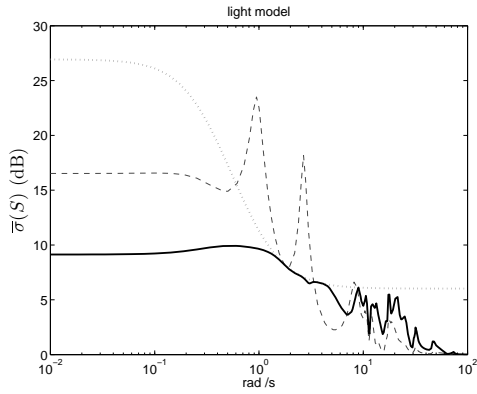
Fig. 7. Largest singular-value of the sensibility function (dashed: initial stabilizing controller, solid: fina controller)

Fig. 8. root-locus analysis ('x': open-loop, '+':closed-loop)

degradation is observed.

Closed-loop system responses for six different load conditions are depicted in Figure 9, more precisely the rigid yaw angle β together with the roll rate p_6, the yaw rate r_6 and the roll angle ϕ_6 measured at the center of the airplane. System responses meet the flyin quality requirements and robust performance has been obtained. Additionally, the closed-loop system clearly satisfie comfort and damping ratio requirements for load conditions.

IV. CONCLUSION

This paper has focused on the design of a fligh controller for the lateral motion of a highly fl xible aircraft subject to exogenous disturbances and different load conditions. A reduced-order feedback controller as well as a static feed-forward controller have been designed simultaneously without recourse to risky order reduction schemes. The study case is a challenging application as it involves a 68th-order plant, several operating conditions and stringent time- and
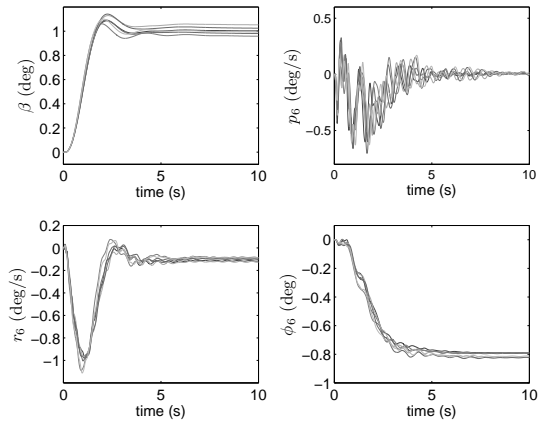
(a) β_r step response
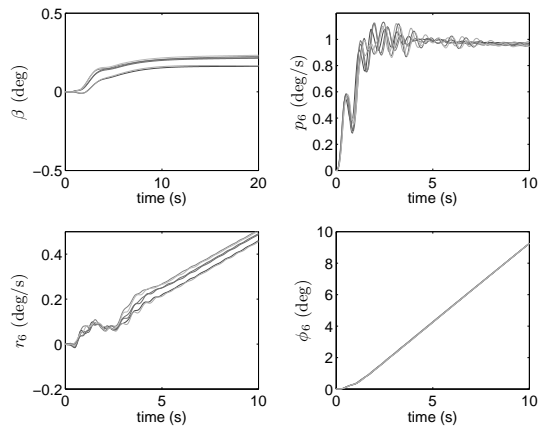
(b) ϕ_r ramp response

Fig. 9. Closed-loop system responses under different load configuration

frequency domain specification in addition to structural constraints on the controller. The proposed nonsmooth optimization technique has been shown to hold promise in solving a set of concurrent constraints and in achieving turbulence attenuation and robustness with respect to fl xible mode uncertainties.

The proposed approach is local in nature which means optimality certificate are local as opposed to the indisputable global certificate We think this is a minor weakness widely offset by the fl xibility to directly cope with multiple specifications Specification are indeed handled as stated in practice by designers thus bypassing conservative embedding as is usually the case with more traditional techniques.

REFERENCES

[1] D. Alazard. Robust H_2 design for lateral fligh control of highly fl xible aircraft. *AIAA J. of Guidance, Control, and Dynamics*, 25(3), 2002.
[2] P. Apkarian and D. Noll. Nonsmooth H_∞ synthesis. *IEEE Trans. Aut. Control*, 51(1):71–86, 2006.
[3] P. Apkarian, D. Noll, and A. Rondepierre. Mixed H_2/H_∞ control via nonsmooth optimization. *SIAM J. on Control and Optimization*, 47(3):1516–1546, 2008.
[4] P. Apkarian and D. Noll. IQC analysis and synthesis via nonsmooth optimization. *Syst. Control Letters*, 55(12):971 – 981, 2006.
[5] G. J. Balas and J. C. Doyle. Control of lightly damped, fl xible modes in the controller crossover region. *Journal of Guidance Control Dynamics*, 17:370–377, March 1994.
[6] V. Bompart, P. Apkarian, and D. Noll. Non-smooth techniques for stabilizing linear systems. *American Control Conference, 2007. ACC '07*, pages 1245–1250, July 2007.
[7] V. Bompart, P. Apkarian, and D. Noll. Control design in the time- and frequency-domain using nonsmooth techniques. *Syst. Control Letters*, 57(3):271–282, 2008.
[8] S. Boyd and C. Barratt. *Linear Controller Design: Limits of Performance*. Prentice-Hall, 1991.
[9] F. H. Clarke. *Optimization and Nonsmooth Analysis*. Canadian Math. Soc. Series. John Wiley & Sons, New York, 1983.
[10] S. Gumussoy and M. L. Overton. Fixed-order H_∞ controller design via HIFOO, a specialized nonsmooth optimization package. *American Control Conference, 2008*, pages 2750–2754, June 2008.
[11] F. Kubica, T. Livet, X. Le Tron, and A. Bucharles. Parameter-robust fligh control system for a fl xible aircraft. *Control Engineering Practice*, 3(9):1209 – 1215, 1995.
[12] M. Merkel, M. H. Gojny, and U. B. Carl. Enhanced eigenstructure assignment for aeroelastic control application. *Aerospace Science and Technology*, 8(6):533 – 543, 2004.
[13] Y. Piguet, U. Holmberg, and R. Longchamp. A minimax approach for multi-objective controller design using multiple models. *Int. J. Control*, 72(7):716–726, may 1999.
[14] E. Polak. *Optimization : Algorithms and Consistent Approximations*. Applied Mathematical Sciences, 1997.
[15] M. Sato and M. Suzuki. Vibration control of fl xible structures using a combined H_∞ filte approach . *AIAA J. of Guidance, Control, and Dynamics*, 19(5):1000–1006, 1996.
[16] A. M. Simões, P. Apkarian, and D. Noll. A nonsmooth progress function for frequency shaping control design. *IET Control Theory & Applications*, 2(4):323–336, April 2008.
[17] M. Tahk and J. L. Speyer. Parameter robust linear-quadratic-Gaussian design synthesis with fl xible structure control applications. *AIAA J. of Guidance, Control, and Dynamics*, 12:460–468, 1989.
[18] R. J. Veillette, J. B. Medanic, and W. R. Perkins. Design of reliable control systems. *Automatic Control, IEEE Transactions on*, 37(3):290–304, Mar 1992.
[19] K. Zhou, J. C. Doyle, and K. Glover. *Robust and Optimal Control*. Printice Hall, 1996.